JAXA-ONERA-DLR Cooperation: Results from Multi-Point Aerodynamic Optimization of a Rotor in Hover and Forward Flight

Joëlle Bailly, Gunther Wilke, Keita Kimura, Yasutada Tanabe

▶ **To cite this version:**

Joëlle Bailly, Gunther Wilke, Keita Kimura, Yasutada Tanabe. JAXA-ONERA-DLR Cooperation: Results from Multi-Point Aerodynamic Optimization of a Rotor in Hover and Forward Flight. 49th European Rotorcraft Forum - ERF 2023, Sep 2023, Bückeburg, Germany. hal-04380533

HAL Id: hal-04380533
https://hal.science/hal-04380533v1

Submitted on 8 Jan 2024

HAL is a multi-disciplinary open access archive for the deposit and dissemination of scientific research documents, whether they are published or not. The documents may come from teaching and research institutions in France or abroad, or from public or private research centers.

L'archive ouverte pluridisciplinaire **HAL**, est destinée au dépôt et à la diffusion de documents scientifiques de niveau recherche, publiés ou non, émanant des établissements d'enseignement et de recherche français ou étrangers, des laboratoires publics ou privés.

JAXA-ONERA-DLR COOPERATION: RESULTS FROM MULTI-POINT AERODYNAMIC OPTIMIZATION OF A ROTOR IN HOVER AND FORWARD FLIGHT

Joëlle Bailly, The French Aerospace Lab ONERA, Meudon, France
Gunther Wilke, German Aerospace Center, Braunschweig, Germany
Keita Kimura, Japan Aerospace Exploration Agency, Tokyo, Japan
Yasutada Tanabe, Japan Aerospace Exploration Agency, Tokyo, Japan

Abstract

The three research organizations, JAXA, ONERA and DLR have decided to combine their efforts in 2019 to compare and improve their own aerodynamic simulation and optimization strategies. The first two work packages of this collaboration involved single-objective optimizations in hovering flight and then in forward flight. The objective of the study presented in this paper is to perform and compare multi-point aerodynamic optimizations combining these two antagonistic flight cases. The optimization procedures are based on surrogate models, generated by low- and high- fidelity simulation codes. Chord and twist distributions are optimized to improve the performance in hover, and the effective lift-to-drag ratio in cruise. The Pareto fronts are generated and three designs are analyzed in details: Best Cruise, Multi-Purpose, and Best Hover. Similar trends are identified for optimum designs obtained by each partner. In hover, the most influential parameter is a negative twist at the tip, to delay stall occurrence at high thrust values. The estimated power benefit in the Best Hover designs is about 5%. For the selected cruise configuration, with a high advance ratio equal to 0.7 (due to a reduced RPM), the Best Cruise designs present a near-zero twist slope and a chord distribution with a thinning at the root and the tip, balanced by a thickening at mid-span, which reduce the effective drag in the advancing side of the blade. The power benefits are about 15%. The Multi-Purpose designs have a blade planform close to the Best Cruise designs. The twist slope is slightly less than the Baseline. The aerodynamic behaviors in hover and cruise are fairly close to those of the Baseline, with a range of performance gains between 1 and 3% in hover and cruise.

1. INTRODUCTION

Helicopters are versatile machines, capable of vertical take-off and landing, hovering, and forward flight. The optimization of helicopter rotor blades poses different challenges, as the problem is multi-disciplinary, multi objectives (often antagonistic) can be considered, and multiple analysis models of varying fidelity levels are available for each discipline.

In this paper, we will focus on a multi-point aerodynamic optimization of a rotor blade in hover and cruise. Each flight configuration has its own physical characteristics and difficulties to be evaluated numerically. Different levels of fidelity of simulation codes, based on lifting line, unsteady aerodynamics, fluid/structure coupling can be used to simulate these types of flows, with increased degrees of accuracy. Given the computational cost of high-fidelity methods, based on CFD simulations, introducing multi-fidelity surrogate models is a solution to limit the number of required simulations in the optimization procedures.

ONERA, DLR and JAXA have independently been working to establish rotor blade optimization methodologies [1][2][3] A first collaborative work was set up between ONERA and JAXA a few years ago [4]. In 2019, the three organizations decided to join their knowledge and expertise on aerodynamic and acoustic simulations and optimizations strategies. The objectives of this collaborative work consist in the comparison, the exchange and the improvement of each partner's best practices to design rotor blades using multi levels of fidelity of surrogate models in the optimization procedures.

The objective of the optimizations is to improve the performance of the reference rotor (BO-105 rotor of HART-II campaign [5]) in hovering flight during Phase 1 of the cooperation [6], then in low RPM forward flight in Phase 2 [7]. The decision variables involve chord and twist laws. The surrogate models used in the optimization procedures are built from

numerical simulations of different levels of fidelity: lifting line type methods for low-fidelity (LoFi), and CFD-RANS or CFD-URANS methods for high-fidelity (HiFi).

The purpose of Phase 3 of this collaboration, presented in this paper, is to consider a multi-point objective function, combining the hover and the forward flight configurations. The Pareto fronts, the evolutions of the design variables and the aerodynamic behaviors of the designs with respect to the different states of the flight, as well as the shapes and the accuracy of the surrogate models will be compared and analyzed.

2. METHODOLOGIES

2.1. Simulation Approaches

The performance of the optimized designs of rotor blades are evaluated by two types of numerical methodologies: a low-fidelity method based on Blade Element Theory, and a high-fidelity method based on Computational Fluid Dynamics. Each partner uses its own simulation methods, with the parameters settings that have been previously validated for each type of flight configuration. Table 1 and Table 2 summarize the characteristics of each partner's low-fidelity and high-fidelity methods.

Table 1: Low-Fidelity methods to evaluate rotor performance.

	ONERA	DLR	JAXA
Code	HOST [8]		rBET
Inflow model	Finite State [9] (Hover) Prescribed wake [10] (Cruise)		Pitt & Peter
Structural adjustment	Polynomial fit [11]	Linear scaling [12]	-

More precisely, for the High-fidelity methods, dealing with CFD simulations, different grid techniques are used by the partners.

ONERA uses a Chimera technique to model a single rotor blade within a quarter cylinder background grid and periodicity boundary conditions for Hover simulations, or an isolated rotor within a Cartesian box for Cruise simulations. A multi-block, deformable mesh of O-H type is generated for the blade mesh, where the root and tip caps are modelled in separate grid blocks. The grids of the new rotor designs are generated through a deformation of the baseline grid, based on a quaternion approach, developed in the in-house QUANTUM [13] code. The background grid is automatically generated using Cassiopee [14], a set of Python modules for pre- and post-processing of CFD computations.

DLR uses its own grid generator G3 (G-cube) based on transfinite interpolation, like GEROS [15]. Thus, a grid is automatically generated for each new rotor design. Here an O-O block is generated with periodic boundaries, which is extended by additional H-O blocks towards the farfield. Like ONERA, the Froude boundary condition is available on the outer mesh for Hover simulations. In forward flight, the Chimera technique is also applied to model all four blades. To enhance the resolution near the blades without increasing the computational cost to much, hanging grid nodes are employed near the Cartesian background grid, which itself is encapsulated in a cylindrical mesh to reach a good farfield distance to avoid reflections.

In JAXA's simulations, rectangular background grids are prepared and a set of overlapping blade grids is placed within them. The calculation proceeds by moving this blade grid at each calculation step. Pointwise was used to create the blade grid, and rGrid, an automatic grid generator provided by JAXA, is used to generate the background grids.

Table 2: High-fidelity methods to evaluate rotor performance

	ONERA	DLR	JAXA
Solver	*elsA* [16]	FLOWer [17]	rFlow3D [18]
Inviscid scheme	2^{nd} order JST [19]	4^{th} order FMCT [20] (vA) [21] + SLAU2 [22]	4^{th} order FMCT [20]+ SLAU2 [22]
	with 2^{nd} order finite volume metric		
Time integration	Dual time Backward Euler scheme + LU-SSOR [23]	Dual time Backward Euler scheme + LU-SSG [24]	Dual time LU-SGS [24](Blade) & 4-stage RK (Background)
Turbulence model	Kok-SST[25] Fully turbulent	SA-DDES-R [26] Empirical laminar-turbulent transition Prediction [27]	SA-R [26] Fully turbulent
Rotor property	Elastic, through data airloads approach with HOST		Rigid

The characteristics of grid dimensions are given in Table 3 for Hover and in Table 4 for Cruise.

Table 3: Grid properties of grids for Hover simulations.

	ONERA	DLR	JAXA
Chordwise	80	128	161
Spanwise	80	128	121
Boundary layer	~35	~30	~40
Wake resolution (%c)	7	10-30	20
Number of cells (1 Blade)	0.44 M	2.1 M	1.2 M
Number of cells (Background)	6.20 M	0.8 M	11 M
Total number of cells	6.64 M	2.9M	16 M

Table 4: Grid properties of grids for Cruise simulations.

	ONERA	DLR	JAXA
Chordwise	80	80	161
Spanwise	80	80	121
Boundary layer	~35	~15	~40
Wake resolution (%c)	7	21	20
Number of cells (4 Blades)	1.75 M	1.0 M	4.4 M
Number of cells (Background)	41.25 M	3.7 M	13 M
Total number of cells	43 M	4.9 M	18 M

2.2. Optimization setup

Optimization procedures

Each partner has developed and validated its own optimization procedure, based on Efficient Global Optimization (EGO) [28] methods. A Kriging surrogate model is generated from a Design of Experiment (DoE) data base, built from an initial data sampling of the research domain. This model is then progressively enriched with the search for the minimum and/or the maximum Expected Improvement (EI) points. The main advantage of surrogate models is the large reduction of computational cost to obtain a final optimized design, especially when high fidelity simulation tools are used. Table 5 briefly summarizes the optimization numerical tools used by each institution.

Table 5: Optimization numerical tools.

	ONERA	DLR	JAXA
Framework	Korrigan[1]	POT[2]	[29][30]
Meta model	Kriging and Co-Kriging [31]	Hierarchical Kriging [32]	Kriging
Optimizer	Genetic Algorithm	Diff. Evolution + Nelder & Mead	Genetic Algorithm

Baseline rotor and flight conditions

The BO-105 rotor defined for the HART-II campaign [33] is the baseline blade, and its specifications are described in Table 6.

Table 6: Characteristics of Baseline blade.

Item	Value
Number of blades	4
Radius (m)	2
c_{ref} (m)	0.121
Linear nose-down twist (°/R)	-8.
Shape	Rectangular
Airfoil	NACA23012

The flight conditions are presented in Table 7. For the forward flight configuration, it is assumed to consider a compound helicopter with a separate lift generator, such as fixed-wings or propellers. The main rotor is set to generate a lift corresponding to 30% of the aircraft's weight. To achieve a high advance ratio, the main rotor is rotated at a lower speed compared to the blade tip speed of conventional helicopters. The shaft axis is set at 0º shaft angle to keep the rotor disk horizontal and reduce the rotor drag during high-speed flight.

Table 7: Flight configurations in Hover and Cruise.

	Hover	Cruise
Thrust (N)	5582	1080
c_T/σ	0.1	0.034 (30% of weight)
Advance Ratio μ	0.	0.7
Minf	0.	0.34
Mtip	0.	0.48
Rotational speed (RPM)	1042	781.5
Shaft angle (°)	0.	0.

When investigating multiple flight conditions with their respective associated goal function, one can either choose to use a weighted objective function or a true multi-objective optimization. For better comparability, a weighed objective function has been used to find a) the best hover, b) the best cruise and c) a balanced Multi-Purpose blade found with the average of the two goal functions. Additionally, ONERA and DLR sought the respective Pareto fronts. Since HiFi simulations are much longer in terms of CPU time, ONERA chose to determine the best designs in Hover and in Cruise. Then, the Multi-Purpose design corresponds to the mid-point of the Pareto Front constructed from the surrogate models generated at the two extreme configurations, thanks to the NSGA-II [34] optimizer. HiFi simulations were then performed a posteriori for this point. On the other hand, DLR and JAXA defined the Multi-Purpose design by using HiFi simulations into their respective optimization procedures. DLR also carried out a true multi-objective optimization with the high- and low-fidelity methods for reference through the application of the sorting algorithm of the NSGA-II with the Differential Evolutionary algorithm.

Design variables and Objective functions

The analysis of the results obtained during the previous Phases 1 and 2 allowed the partners to better define the choice of the most influential decision variables for the improvement of the performance according to the flight configurations, as well as their definition domains. A total of four variables is applied, two for the chord, and two for the twist distributions. Furthermore, the chord distribution is weighted to maintain a constant thrust weighted solidity (Eq. 1):

$$(1) \quad \boldsymbol{c_{ref}} = \frac{\int_0^R \boldsymbol{c(r) r^2 dr}}{\int_0^R \boldsymbol{r^2 dr}}$$

where *c* is the chord length at the radial position *r* and *R* is the blade radius.

The twist spline is applied as Δ-form, which means it is added to the linear twist, whose value is itself optimized. The twist is set at zero at r/R=0.75.

Table *8* summarizes the definition domains of the different decision variables.

Table 8: Design variables.

Name	Variables settings	Range
chord1	chord @ r/R=0.8	1.0~1.5 c_{ref}
chord2	chord @ r/R = 1.0	0.5~1.0 c_{ref}
dt	dt	-10°~0°
dtwist2	dθ2 @ r/R = 1.0 (from 0.875)	-5°~5°

For the hover configuration, the objective function is the maximization of the figure of merit, defined in Eq.2 as:

$$(2) \quad FM = \frac{C_T^{3/2}}{\sqrt{2} C_Q}$$

with C_T and C_Q being the thrust and torque coefficients of the rotor. As the rotor is trimmed to a prescribed thrust, the objective is the same as minimizing the required power.

The objective function for the forward flight configuration is the improvement of the effective lift-to-frag ratio L/D_e (Eq. 3), where L is the rotor lift, D is the wind-axis drag force, P is the power of rotor and V is the flight speed.

$$(3) \quad L/D_e = \frac{L}{D + P/V}$$

Actually, D_e represents the induced and the profile drag terms, without considering the propulsive part of the rotor, ensured by other devices, such as propellers. As the rotor is trimmed at prescribed thrust, the objective function corresponds to the minimization of the effective drag term.

When considering practical design, both hovering and forward flight performance must be balanced. Generally, there exists a trade-off relationship between hovering performance and forward flight performance, necessitating strategic design techniques to maintain a balanced optimization. This study proposes to achieve this by considering the assumed mission of the design aircraft. The hovering power, P_{hv}, and the forward flight power, P_{FF}, are calculated and weighted based on the flight time under each flight condition (t_{hv} and t_{FF}), enabling optimization using a single objective function referred to as the total mission power, E_{total}. The equations and conceptual diagram are shown in Equations 4 and 5, as well as Figure 1. Here, *ω* represents the rotor's angular speed and *V* denotes the forward speed. In

this study, conditions where the hovering time and forward flight time are in a 1:1 ratio are referred to as 'Multi-purpose' conditions.

(4) $$E_{total} = P_{hv}t_{hv} + P_{FF}t_{FF}$$

(5) $$\begin{aligned} P_{hv} &= Q_{hv}\omega_{hv} \\ P_{FF} &= DV_{FF} + Q_{FF}\omega_{FF} \end{aligned}$$

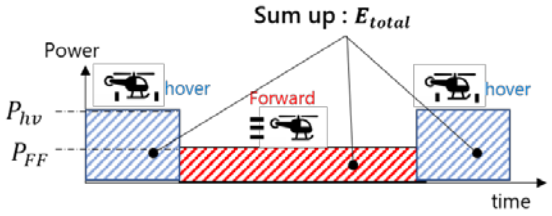

Figure 1: Concept of total power consumption of the mission

3. ANALYSIS OF BASELINE RESULTS

The first step to evaluate the accuracy of the LoFi and HiFi methodologies set up by each partner is to compare the power consumption and the pitch control angles, evaluated for the Baseline, for the Hover and the Cruise configurations. The performances evaluated by LoFi and HiFi simulations are given in Figure 2, for the Hover and Cruise configurations.

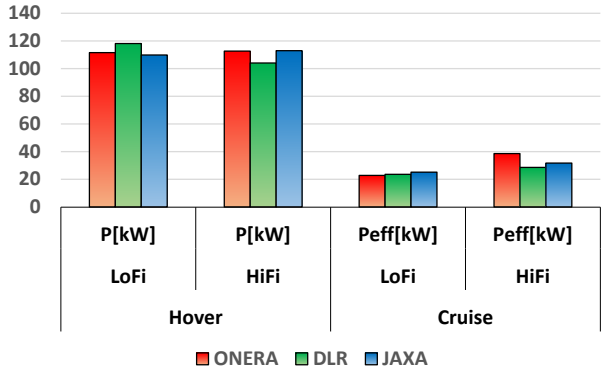

Figure 2: Evaluations of power consumption in Hover and Cruise - LoFi / HiFi

The power evaluations are of the same order of magnitude for the three partners. The almost similar low-fidelity trends of DLR and ONERA is attributed to the utilization of the same comprehensive codes with minor differences in the utilization.The lower power consumption of power by the DLR HiFi results is attributed to the inclusion of laminar-turbulent transition prediction. It has been checked that especially on the lower blade surface (pressure side) large laminar flow regions are possible up to the airfoil tab, but also somewhere around 20% laminar flow on the suction side is observed. Opposing this, the fully turbulent high-fidelity simulations by ONERA and JAXA results match well.

The control pitch angles are given in Figure 3 for the Hover configuration and in Figure 4 for the Cruise.

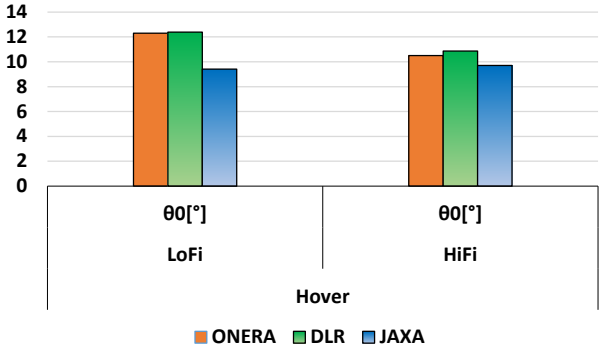

Figure 3: Comparison of collective pitch angle in Hover – LoFi / HiFi

For the Hover case, we can notice an underestimation of the collective pitch for LoFi JAXA simulation, which can be due to rigid blade simulation, and an arbitrary induced flow distribution compared to ONERA and DLR LoFi simulations, which simulate a soft blade, and a finite state wake model. The differences are largely reduced with HiFi simulations, as the aerodynamic wake modeling is contained in the 3D Navier-Stokes equations.

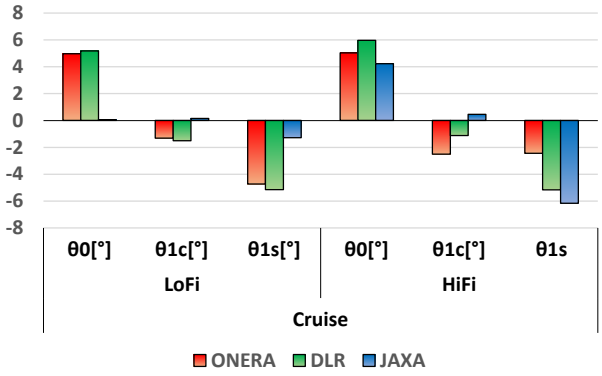

Figure 4: Comparison of collective and cyclic pitch angles in Cruise - LoFi / HiFi

For the Cruise configuration, the control angles determined by the LoFi and HiFi simulations are globally in good agreement between partners, with the exception of the JAXA LoFi simulations for the same reasons as for Hover (rigid blade assumption, and

different induced velocity model). The discrepancies are largely reduced with HiFi simulations.

4. LoFi AND HiFi OPTIMIZATION RESULTS

4.1. Geometrical laws and blade planforms

Three optimized designs will be studied in particular: the one obtained for the hovering flight (Best Hover), the one obtained for the forward flight (Best Cruise), and the one obtained as a compromise with an even weight between the two flight configurations (Multi-Purpose). LoFi simulations being low-time consuming, the three partners defined these three best designs using simulations in their respective optimization procedures.

The chord distributions for the three best designs, obtained by LoFi and HiFi methods are presented and compared in Figure 5. The LoFi designs obtained by the three partners are similar. For the Best Cruise designs, the chord length at mid-span is thicker than the reference, while it is reduced at the blade root and the blade tip (effect of the constraint on the chord to maintain a constant thrust weighted solidity). The chord evolutions of the Multi-Purpose designs are similar to those of the Best Cruise, except for the DLR, for which the internal part of the chord law remains unchanged – this design tends a bit more hover already. The Best Hover designs feature a thickened chord law at the root, which remains almost constant, and then the blade is tapered at the tip. The HiFi designs have similar characteristics on chord evolutions than LoFi ones. It can be noticed that the Best Cruise rotors have less blade thickening in the mid span, compensated by less taper at the blade tip than LoFi rotors. The chord reduction at the root is a bit higher for DLR than for JAXA and ONERA. The chord evolutions for the Multi-Purpose are now similar for the three partners, with the same chord reduction at the root. For the Best Hover, the chord evolutions at the root and the tip are less pronounced than for LoFi designs. Surprisingly, the JAXA design does not follow the ONERA and the DLR trends. The results between ONERA and DLR are in particularly good agreement for chord evolutions with HiFi methods.

Similar trends between partners' designs are observed for the twist distributions in Figure 6, especially for the LoFi optimizations. Globally speaking, the slope of the twist in the inner part of the blade is lower the closer we get to the forward flight configuration. The twist at the blade tip decreases to large negative values when we tend to hover. The HiFi methods produce the same trends for ONERA and DLR. The Best Cruise designs present a near-zero slope up to 0.875R, then a slight decrease in twist at the blade tip. For the Multi-Purpose designs, the negative twist at the blade tip is more accentuated, being 2° lower with HiFi than with LoFi methods. The slope in the inner part is reduced for HiFi methods (-4.6°/m) compared to LoFi (-7.5°/m). It is a bit surprising that the JAXA designs do not follow the same trends, but agrees better with their LoFi counterparts. The slope of the Best Cruise design is equal to -5.4°/m. For the Multi-Purpose design, the linear slope is increased to -9.7°/m. The slope is rather equal to -8°/m for the Best Hover, while it reaches the maximum limit of -10°/m for ONERA and DLR. These differences could be probably explained by the fact that JAXA simulations consider rigid blades, while ONERA and DLR take into account the elasticity of the blades. Nevertheless, the values of the twist at the blade tip are similar for the three partners. The Best Hover designs present the lowest value of twist possible to be reached (-7°). For ONERA, this value is slightly more negative for HiFi method than for LoFi. The linear slope is slightly increased compared to the Baseline for ONERA and DLR, and rather similar to the Baseline for JAXA.

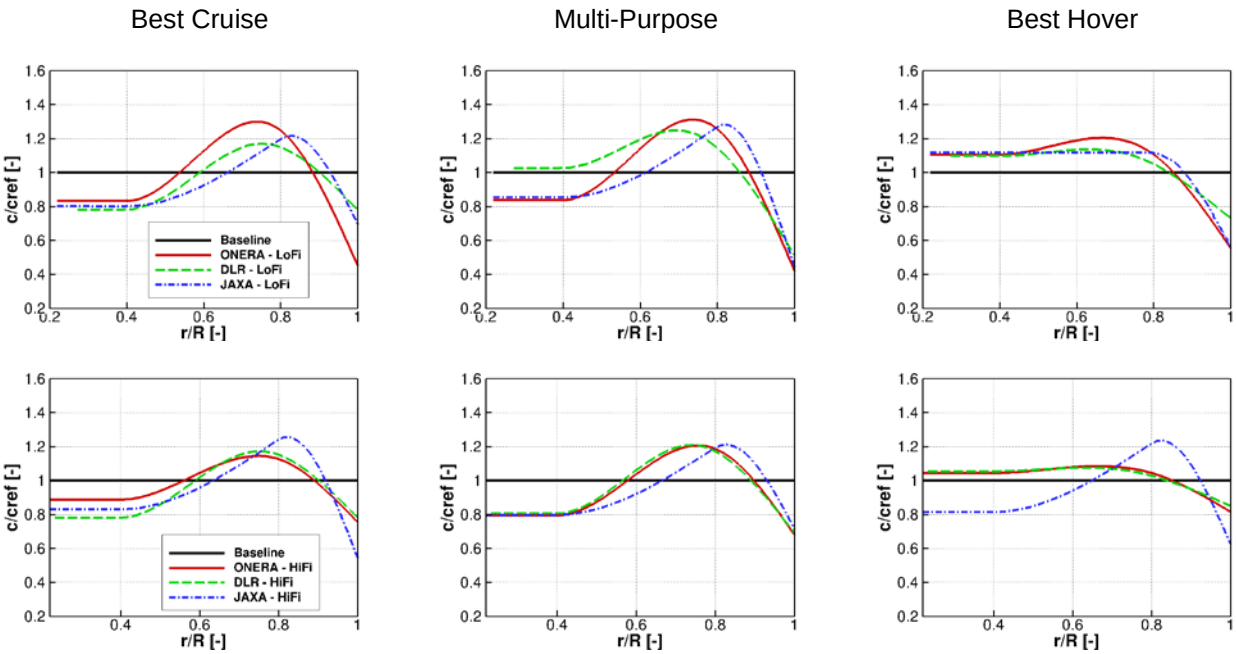

Figure 5: Chord distributions of optimized blades - LoFi / HiFi.

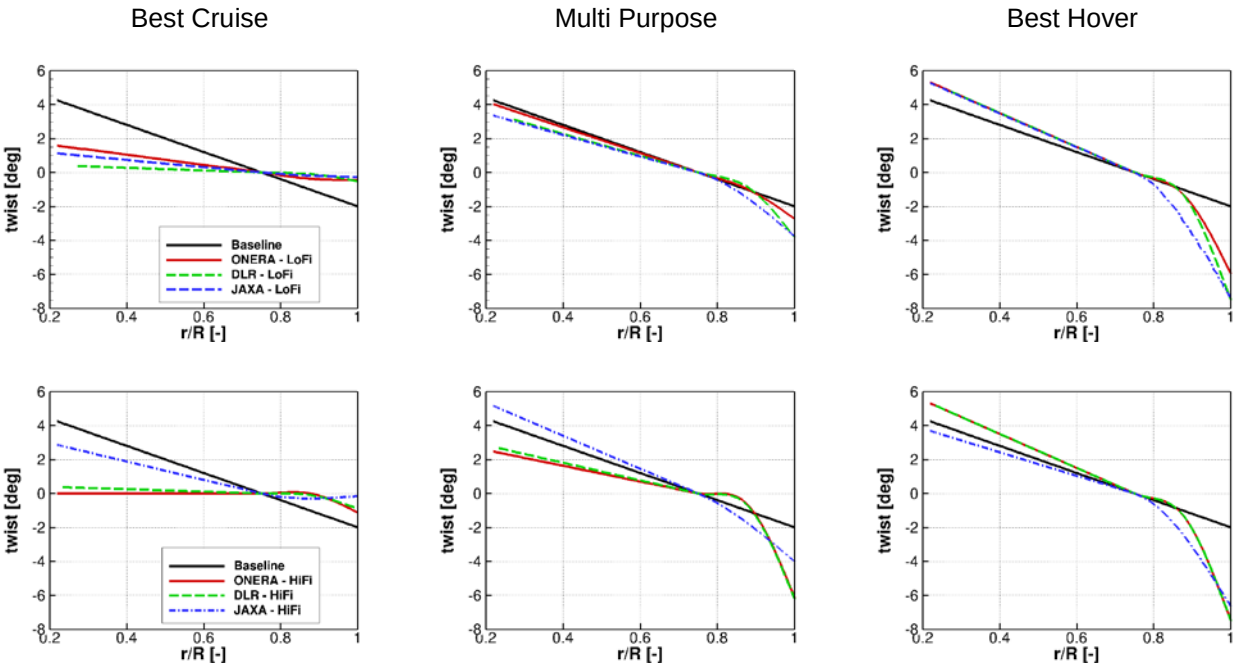

Figure 6: Twist distributions of optimized blades - LoFi / HiFi

The planforms of the best designs obtained by LoFi and HiFi optimizations are shown and compared respectively in Figure 7 and Figure 8. Generally speaking, the blades become larger at mid-span for the Best Cruise, and the Multi-Purpose designs. The blade tips are tapered for the Best Hover designs.

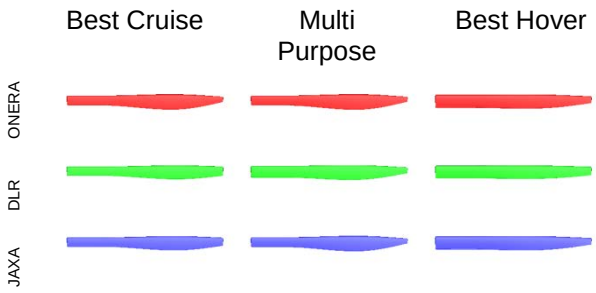

Figure 7: Planforms of optimized blades – LoFi

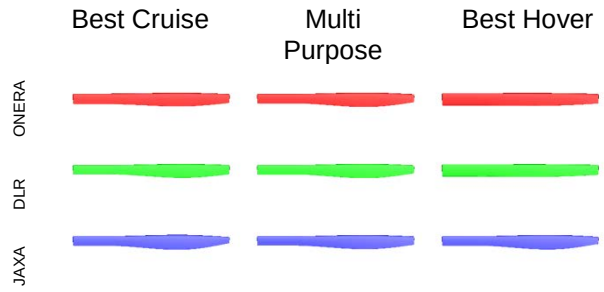

Figure 8: Planforms of optimized blades - HiFi

Table 9 and Table 10 summarize the performance benefits (negative values) or deficits (positive values) with respect to the baseline, respectively in Hover and in Cruise, obtained for the three optimized designs for each fight configuration. The performance of the LoFi (resp. HiFi) designs are evaluated with the LoFi (resp. HiFi) simulation tools.

Table 9: Performance in Hover of optimized blades (LoFi / HiFi)

ΔP Hover (%)	Best Cruise		Multi Purpose		Best Hover	
	LoFi	HiFi	LoFi	HiFi	LoFi	HiFi
ONERA	+3.7	+15.3	-0.8	-0.9	-3.2	-5.9
DLR	+7.0	+12.5	-4.4	-3.7	-6.9	-6.1
JAXA	+15.2	+12.2	-6.7	-3.1	-11.7	-5.0

Table 10: Performance in Cruise of optimized blades (LoFi / HiFi)

ΔPCruise (%)	Best Cruise		Multi Purpose		Best Hover	
	LoFi	HiFi	LoFi	HiFi	LoFi	HiFi
ONERA	-8.8	-15.4	-0.9	-6.0	+24.9	+19.5
DLR	-9.3	-19.0	+1.6	-2.4	+33.8	+24.9
JAXA	-14.7	-9.8	+4.2	-3.4	+77.7	+5.6

Overall, for all patterns and optimization methods combined, performances for Best Hover designs are improved by about 5% in hover, and degraded by between 10 and 20% in cruise. Performances of Best Cruise designs are improved by between 7 and 15% in cruise, and degraded by between 20 to 25% in hover. The range of performance benefits for the Multi-Purpose designs is between 1 and 3% fom HiFi simulations.

The Pareto fronts obtained by the three partners are shown in Figure 9 for LoFi and HiFi methods.

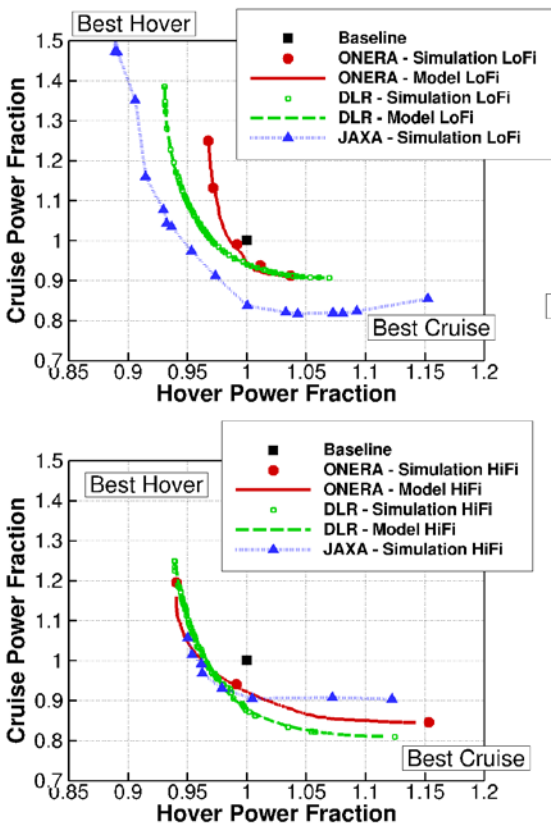

Figure 9: Pareto Fronts – LoFi / HiFi

For LoFi methodologies, there are quite significant differences in performance ratios along the Pareto front, between JAXA's results on the one hand, and those of DLR and ONERA on the other. However, it is not easy to differentiate the effect of aerodynamic modeling (BEMT in rBET for JAXA, and the lifting line/prescribed wake in HOST for ONERA and DLR), from the effect of different optimized blade geometries, particularly concerning the chord evolutions. Towards the Best Cruise design, despite different planforms, performance ratios become similar. The effect of chord laws therefore seems less noticeable than in hover. For HiFi methods, the gaps between the three Pareto fronts are well reduced, especially towards the Best Hover. This shows that the twist law predominates the hover performance. Cruise performance ratios towards Best Cruise show slight differences between ONERA and DLR. The effect of the different blade thinning at the root is more noticeable here. Cruise performance ratios are constant for JAXA, from the middle of the Pareto front (Multi-Purpose) to the Best Cruise. This is probably due to the fact that the linear slope of the twist is greater for JAXA than for DLR and ONERA, which degrades rotor performance towards Best Cruise.

Finally, the DLR results show that, at convergence, the Pareto fronts determined by calculations on the one hand, and by reduced models on the other, are similar. Also, the DLR Multi-Purpose design is also a dominating design, therefore part of the Pareto front, yet it has not been found by the weighted single-objective function approach. The cost is roughly halved when calculating as not the whole front needs to be discovered and may pose a viable alternative to full multi-objective optimizations in the scenario. Unfortunately, a guarantee cannot be given without having searched for the full Pareto front. For ONERA, the multi-purpose point, calculated a posteriori by HiFi simulations, is correctly located on the Pareto front, generated from the surrogate models. The accuracy of the model compared with the HiFi calculation is 0.2% in hovering flight, and -0.6% in forward flight.

We have previously noticed that twist laws have a predominant effect over chord laws on the performance in hover, but also in forward flight. Figure 10 and Figure 11 represent the parameter sensitivity of ONERA and DLR models with respect to the chord and the twist variables seen from their respective best designs. These plots have been generated using the HiFi surrogate models from the optimization, and may not capture the exact values that are further away from the optimum, but should nevertheless reflect the functional trends of these parameters sufficiently well. It has been checked that similar trends are obtained with the LoFi models.

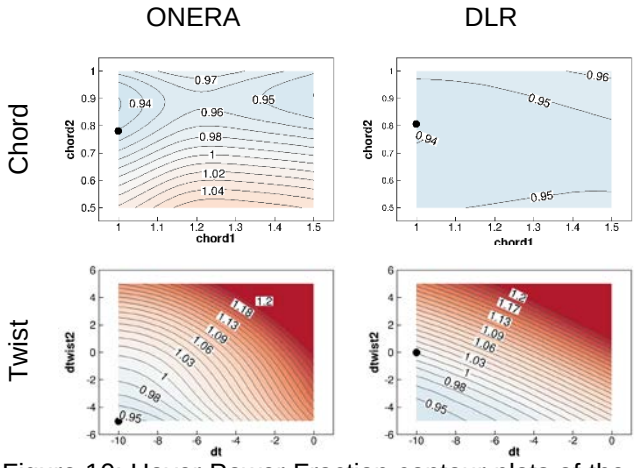

Figure 10: Hover Power Fraction contour plots of the HiFi surrogate models through the Best Hover designs.

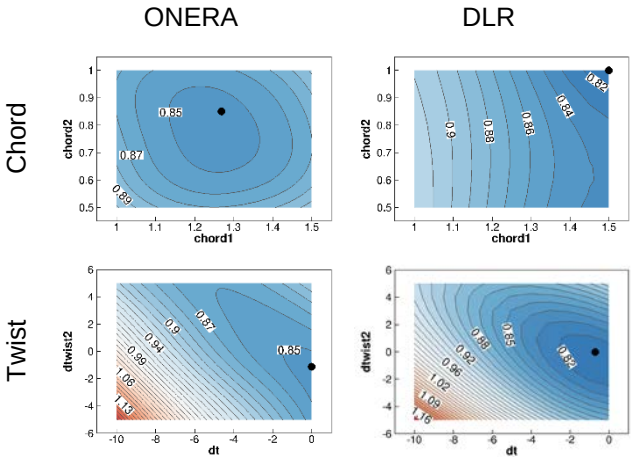

Figure 11: Cruise Power Fraction contour plots of the HiFi surrogate models through the Best Cruise designs.

The agreement is better for the twist parameters. The topology of the models provides well-defined gradients between the areas of loss and benefits of power ratio, in hover and in cruise. The detection of the global minimum point is almost guaranteed. This is why the ONERA and DLR optimization procedures provided very similar twist laws. On the contrary, the landscapes of the contour plots for the chord parameters are much flatter, the gradients of the power ratios are smaller. It is so more difficult to converge to a similar minimum point, which can change with respect to the sensitivity of the numerical codes and the optimizers, e.g. DLR computed laminar-turbulent flow, whereas ONERA computed fully turbulent flow. Besides the shallow gradients, this explains the larger scattering of the optimized chord laws. Likely, the application of the same thrust weighted solidity also leads to the flat landscape for the chord length.

4.2. Analysis of optimized rotors in Hover (HiFi)

The aerodynamic behaviors in Hover of the three optimized designs will be compared and analyzed. These analyses will only be presented on the HiFi best designs, with data from HiFi simulations. It has been checked that similar trends are obtained on the LoFi designs evaluated with LoFi codes. Figure 12 shows the comparison of the radial evolutions of the sectional lift coefficient at the nominal thrust c_T/σ of 0.1, obtained by the three partners.

For the three partners, the Best Hover rotors show a reduction of the amplitude of the lift peak at the blade tip compared to the reference, due to the lower intensity of the tip vortex impacting the blade, which results in improved performance. Conversely,

we can notice an increase of the peak amplitude for the Best Cruise designs. For the Multi-Purpose designs, the impact of the tip vortex is located slightly further inside the blade.

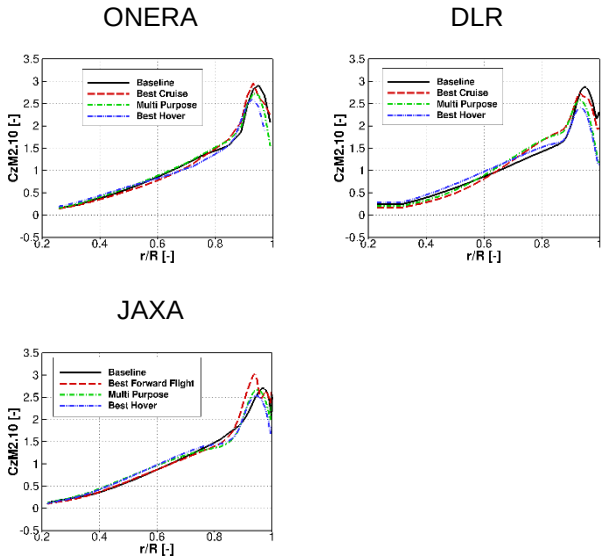

Figure 12: Loads distribution in Hover - c_T/σ=0.1 - HiFi

The evolutions of the Figure of Merit versus the thrust coefficient for the Baseline and the three optimized rotors are compared between the partners in Figure 13. It clearly appears that all partners' HiFi simulations predict an increase of the Figure of Merit at the nominal point (c_T/σ=0.1) for the Best Hover designs. This improvement is evaluated at +4.4% for ONERA, +7.3% for DLR and +5.7% for JAXA. These values are in good agreement with the performance benefits estimated for hover (Table 9). Furthermore, we can notice a delay for the occurrence of stall, which appears around c_T/σ=0.12.The three partners predict a rather early stall for the Best Cruise designs, at c_T/σ of 0.08, with a decrease of the Figure of Merit between 10.6% and 14%, which corresponds to the order of magnitude of performance loss (Table 9). The performances of the Multi-Purpose designs are slightly better than the Baseline by about 3% for DLR and JAXA.

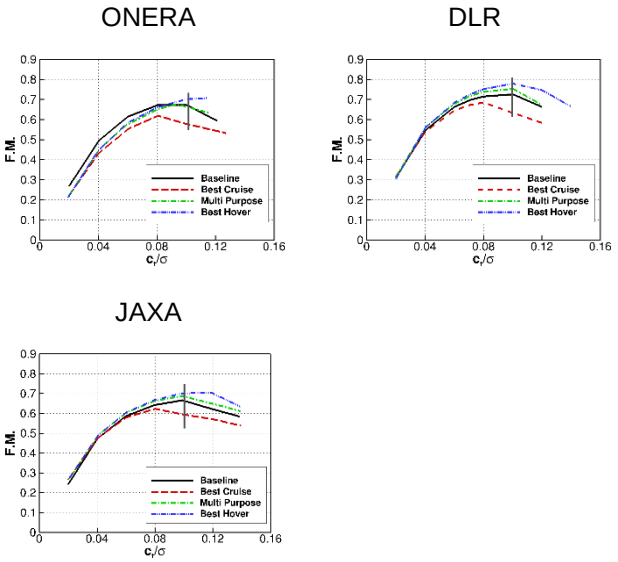

Figure 13: Figure of merit polars – HiFi.

The visualizations of the flowfield, at the nominal thrust c_T/σ of 0.1, around the baseline and the three optimized blades are compared between the three partners in Figure 14. The previous analysis on loads and Figure of Merit are corroborated by the effect of the tip vortex interacting with the different blades. We clearly see that the flow is detached at the tip of the Best Cruise designs, which explains the drop of the Figure of Merit values. The geometry and the twist distribution of the Best Hover and Multi-Purpose optimized blades allow a reduction of the skin friction area on the upper surface of the blade tip, which contributes to improve the performance.

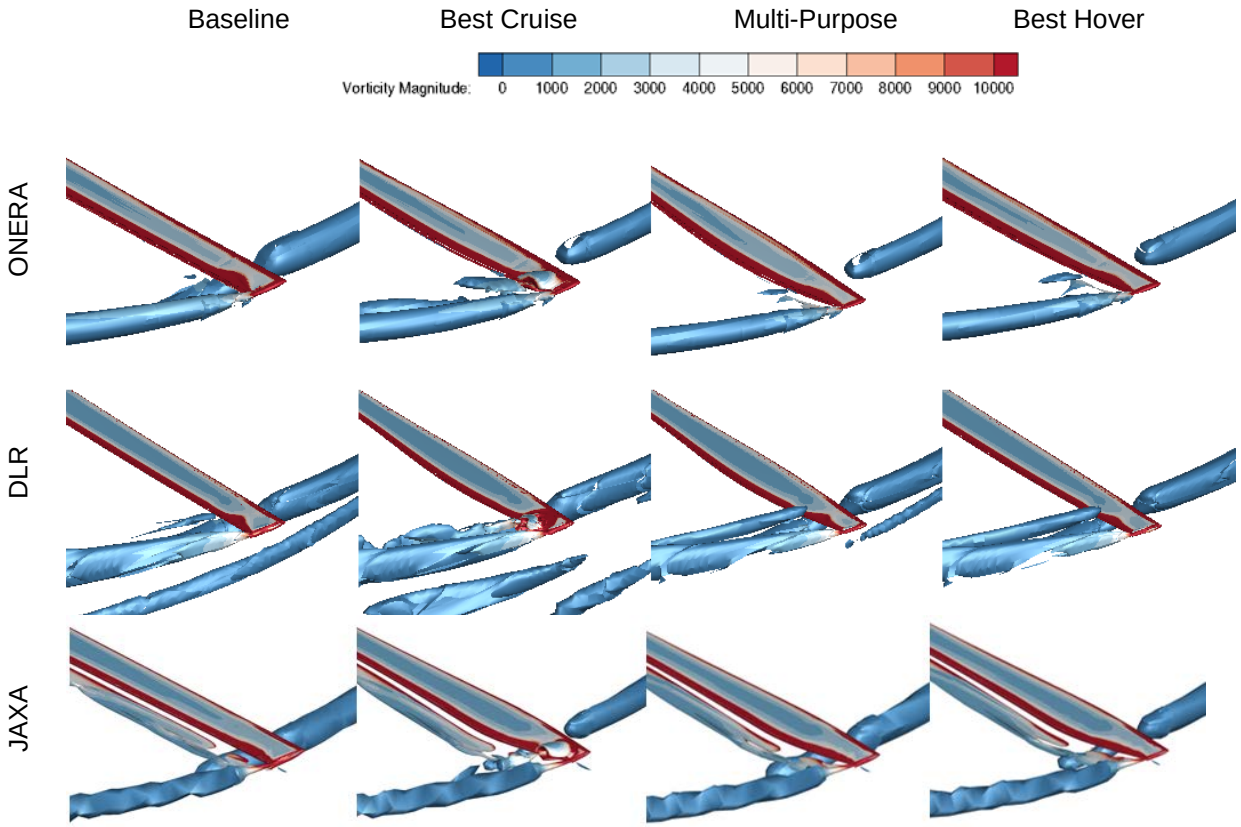

Figure 14: Q-criterion colored with vorticity magnitude - c_T/σ=0.1 - HiFi

4.3. Analysis of optimized rotors in Cruise (HiFi)

The analysis of the aerodynamic behaviors of the three optimized blades, at the nominal design point (μ=0.7, c_T/σ=0.034), are presented, from the HiFi computational results (HiFi best designs evaluated with HiFi simulatons). It has been checked that comparable trends are obtained with the LoFi simulations on LoFi designs. An original way to study the behavior of the different designs is to average the thrust coefficients as a function of azimuth. This is what is done in Figure 15 for the lift coefficients.

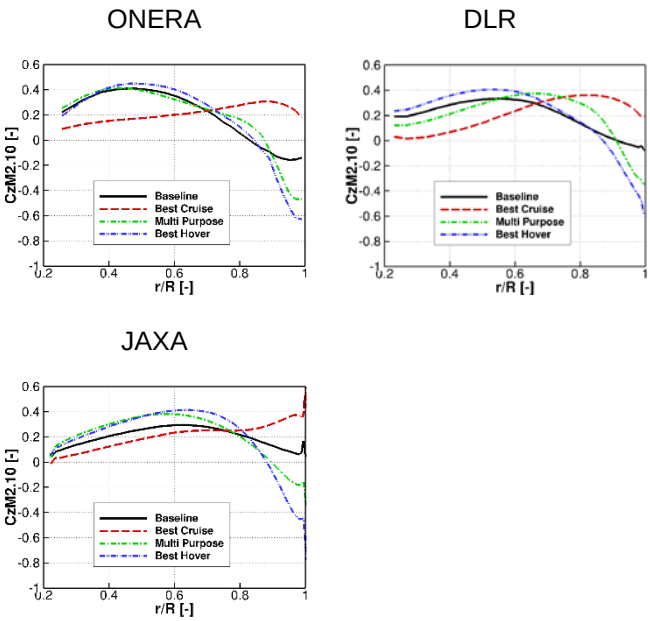

Figure 15: Azimuth-averaged load distributions - (μ=0.7, c_T/σ=0.034) – HiFi

It is clear to all three partners that the lift distribution of the Best Hover design is not suitable for the cruise configuration, especially in the blade tip area. The

loads are largely negative in comparison with the Baseline, which leads to performance degradation (estimated in Table 10). In contrast, the load distribution of the Best Forward Flight blade is much more homogeneous over the entire blade sections. The Multi-Purpose design lies somewhere in between.

In the same manner as what was done for the loads, Figure 16 shows the averaged effective drag coefficient as a function of azimuth versus the radial section. We have previously established that performance optimization is achieved by minimizing the effective drag.

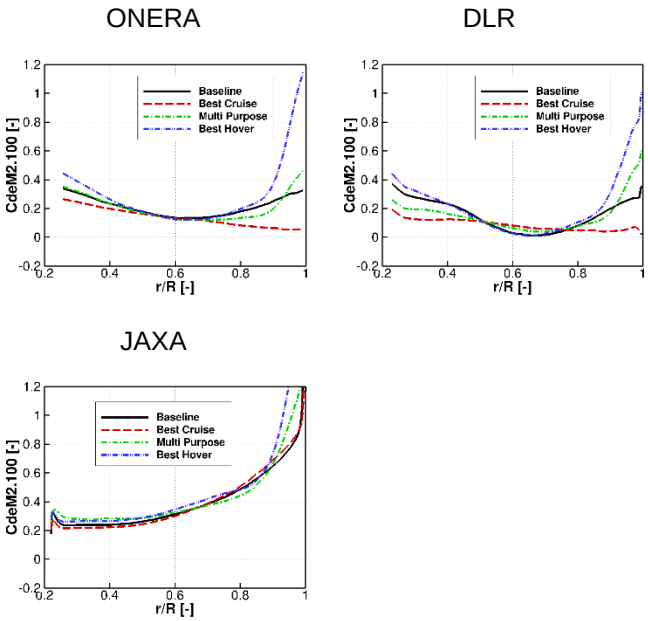

Figure 16: Azimuth-averaged effective drag - (μ=0.7, c_T/σ=0.034) - HiFi

The Best Cruise designs, defined by ONERA and DLR, allow for a significant reduction in this variable, in the inner part (up to 0.4R) and in the outer part (from 0.7R) of the blade. On the other hand, the Best Hover designs result in a very large increase in the effective drag at the outer part of the blade. The Multi-Purpose designs are between these two evolutions. The JAXA designs follow these same trends to a lesser extent. The fact that the variation in the slope of the twist of the three optimized rotors is less pronounced for the JAXA results than for those of ONERA and DLR may explain these differences.

We can have a better idea of the load distributions on the rotor disk, for the Baseline and the three optimized designs, at the nominal design point, in Figure 17. The rotor rotates counter-clockwise, the wind come from the left.

For the considered high advance ratio configuration, the Baseline rotor experiences a load imbalance between the right ($45° \leq \psi \leq 180°$) and the left ($225° \leq \psi \leq 0°$) areas of the rotor disk. The optimized geometry of the Best Cruise designs, defined by the three partners, provides better load distribution between the front ($135° \leq \psi \leq 225°$) and rear ($315° \leq \psi \leq 45°$) of the rotor disks, considering the balance of rolling moment. Conversely, the Multi-Purpose and the Best Hover designs accentuate the imbalance of loads between the right and the left areas. There is an accentuated area of negative loads at the tip of the advancing side of the blade ($90° \leq \psi \leq 120°$), balanced with an accentuated area of positive loads in the internal part of the blade.

The effective drag coefficient distributions on the rotor disk are plotted in Figure 18, for the Baseline and the three optimized designs. As previously observed, for ONERA and DLR, the most important reduction of effective drag occurs near the blade tip, and in the inner part of the advancing blade of the Best Cruise designs, which explains the significant power benefits in Cruise (Table 10). For the Multi-Purpose designs, the effective drag distributions are almost similar to the Baseline. Large increase of the effective drag is observed for the Best Hover designs, leading to a loss of performance (Table 10). For JAXA, the differences between the three optimized blades and the Baseline are less pronounced.

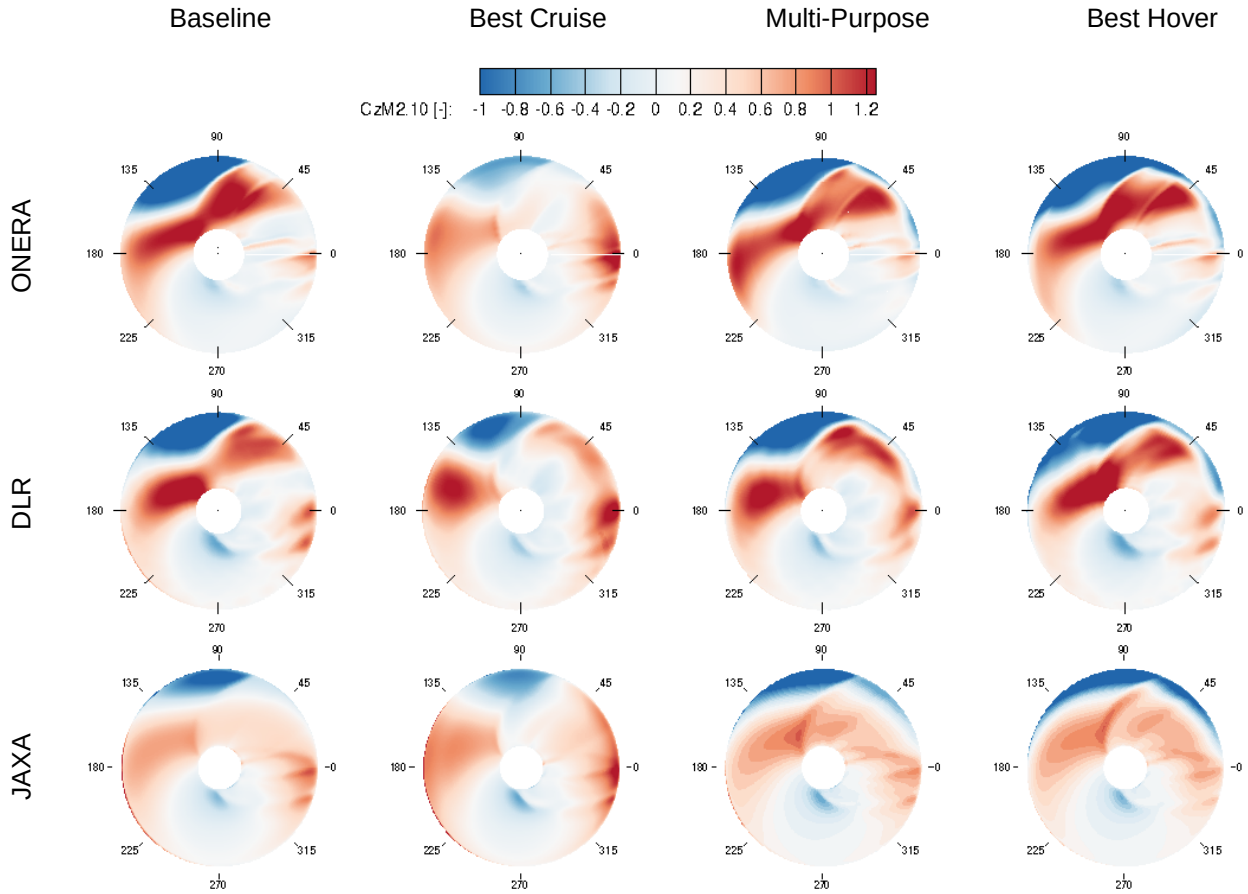

Figure 17: Thrust distribution on the rotor disk - (μ=0.7, c_T/σ =0.034) – HiFi

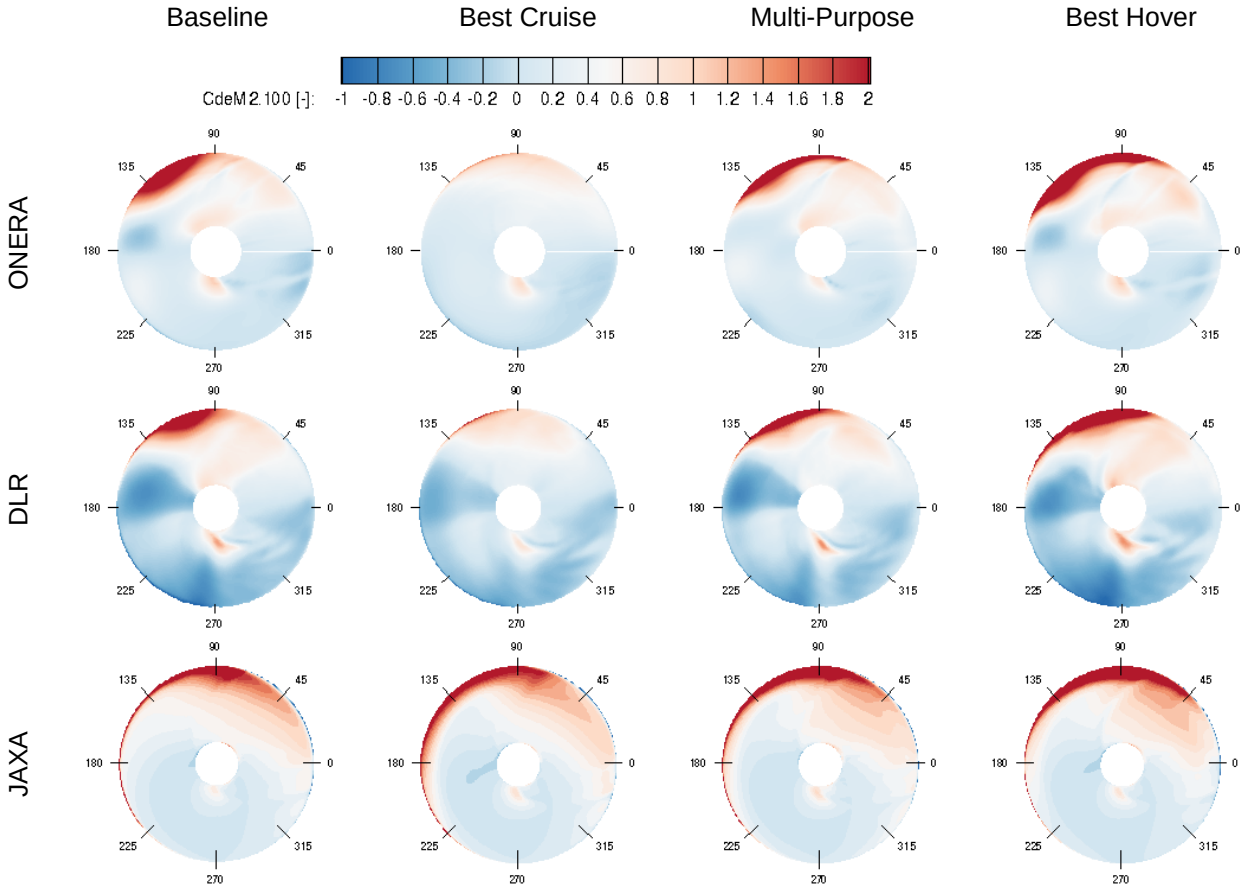

Figure 18: Effective drag distribution on the rotor disk - (μ=0.7, c_T/σ =0.034) – HiFi

Finally, it is interesting to visualize the flowfield, and the structure of the wake developed around the blades of the Baseline, and the three optimized designs, at the nominal design point, in Figure 19.

The Best Cruise designs generate a wake with much lower vorticity intensity than the Baseline. This is particularly noticeable in the intensity of the tip vortices generated in the advancing side. The vorticity of the shear layer is also much reduced. This distribution of vorticity has beneficial effects on the load and drag on one hand, and on the performances on the other hand of Best Cruise designs. The vorticity intensity of the wake generated by the Multi-Purpose designs increases compared with the Best Cruise designs, and is similar to that of the Baseline. Finally, Best Hover wakes have a much higher vorticity intensity, which explains the increased load variation on the rotor disk and the degradation in performance. All these trends are less pronounced for JAXA designs than for ONERA and DLR ones. The presence of the fuselage in the DLR calculations has an influence on the location of the interaction of the tip vortex generated by the forward blade on the following blade, which is located further outside the blade than in the ONERA and JAXA simulations, which consider an isolated rotor.

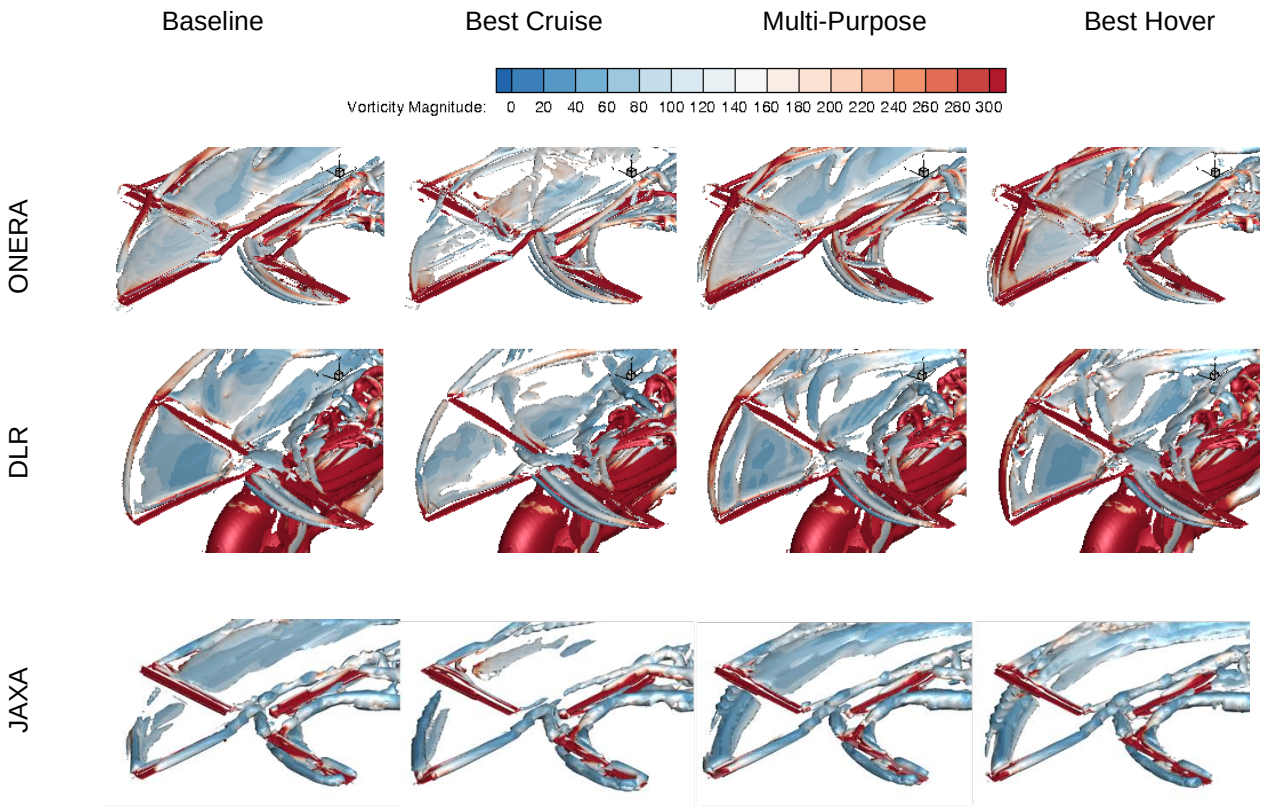

Figure 19: Q-criterion colored with vorticity magnitude - (μ=0.7, c_T/σ=0.034) – HiFi

4.4. Effect of advance ratio variations (LoFi)

It is interesting to evaluate the performance in terms of effective lift-to-drag ratio as a function of the advancing ratio μ, from 0.3 to 1.0, for the Baseline and the three LoFi best designs defined and evaluated with LoFi simulation tools, as shown in Figure 20.

Generally speaking, for the three partners LoFi simulations, the performance in terms of L/D_e ratio is improved with respect to the Baseline for the Best Cruise design, is similar to the Baseline for the Multi-Purpose design, and is largely degraded for the Best Hover design, whatever the value of the μ parameter.

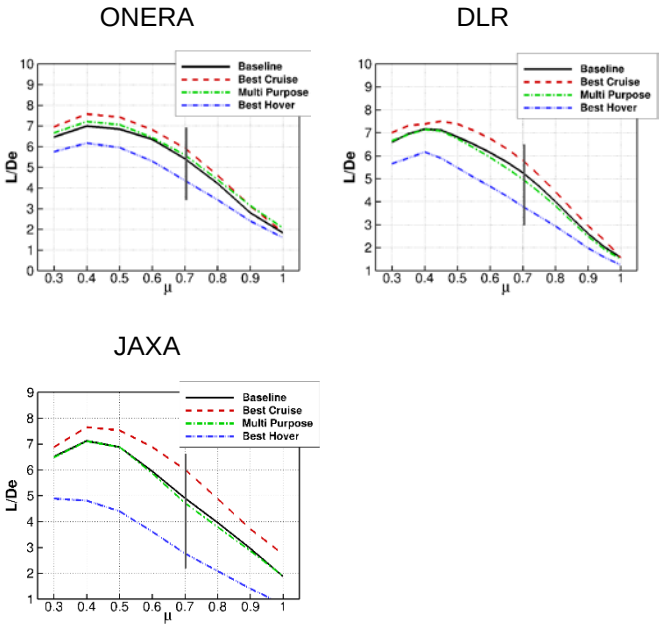

Figure 20: Effect of advance ratio on effective lift to drag ratio – LoFi

The origins of these evolutions can be explained with the distribution of the lift coefficient on the rotor disk, simulated with the ONERA LoFi code, in Figure 21, for three values of the μ parameter: 0.3, 0.7 (nominal value for the optimization), 1.0. It has been checked that the DLR LoFi numerical simulations

provide very similar results, as the two partners use the same comprehensive analysis code, HOST, with similar numerical parameters.

For the three values of μ, it clearly appears that the Best Cruise design allows a better distribution of the loads between left and right on the one hand, and rear and front of the rotor disk on the other hand. As the μ parameter increases, the negative peak of the lift coefficient becomes important, near the blade tip of the advancing side ($60° \leq \psi \leq 120°$).

The distributions of the effective drag on the rotor disk are plotted in Figure 22, for the Baseline, and the three LoFi best designs, for the three values of μ parameter. For the Best Cruise designs, the effective drag coefficient is clearly reduced at the tip of the advancing side for the μ parameters of 0.4 and 0.7. This is not noticeable for μ equal to 1. As the μ parameter increases, the extent and intensity of the inversion circle is growing.

It would be interesting to confirm these trends with HiFi simulations for the HiFi designs.

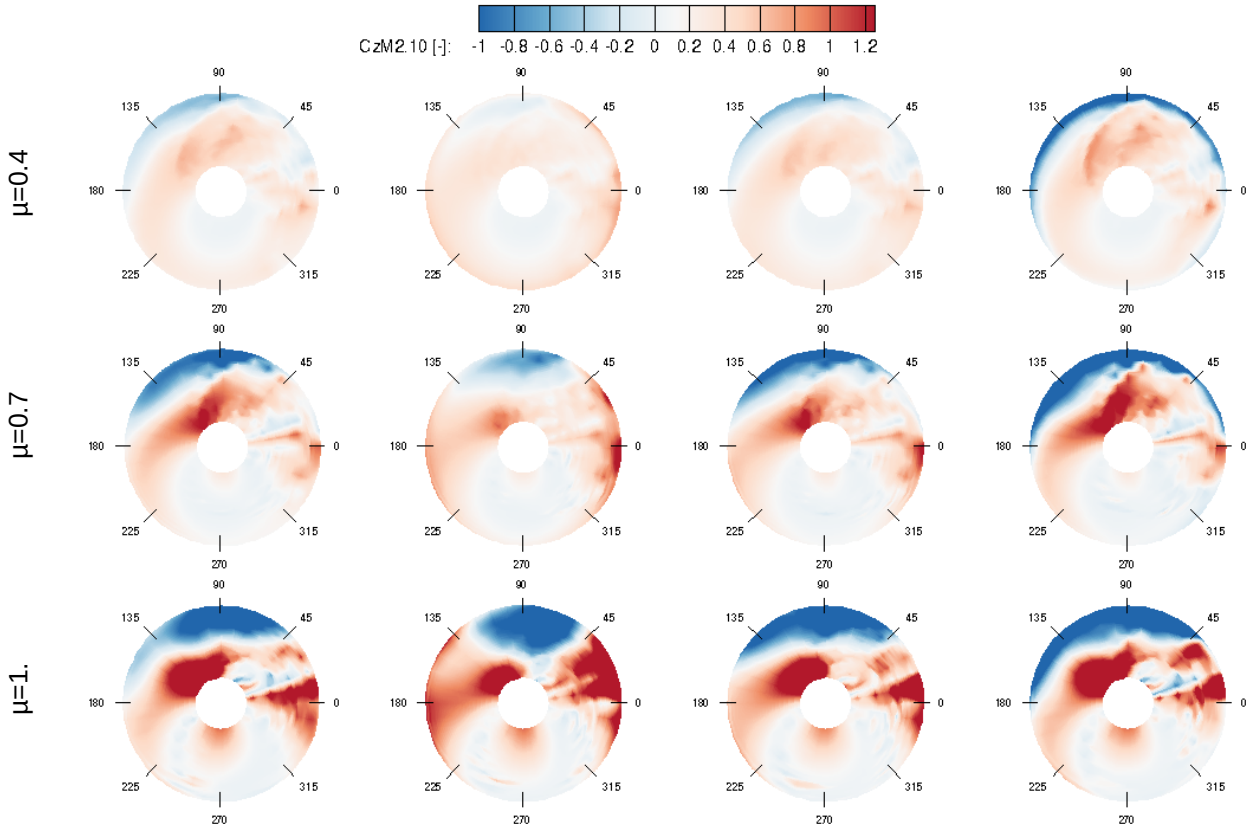

Figure 21: Effect of advance ratio on thrust distribution on the rotor disk – c_T/σ =0.034 - LoFi –ONERA simulations

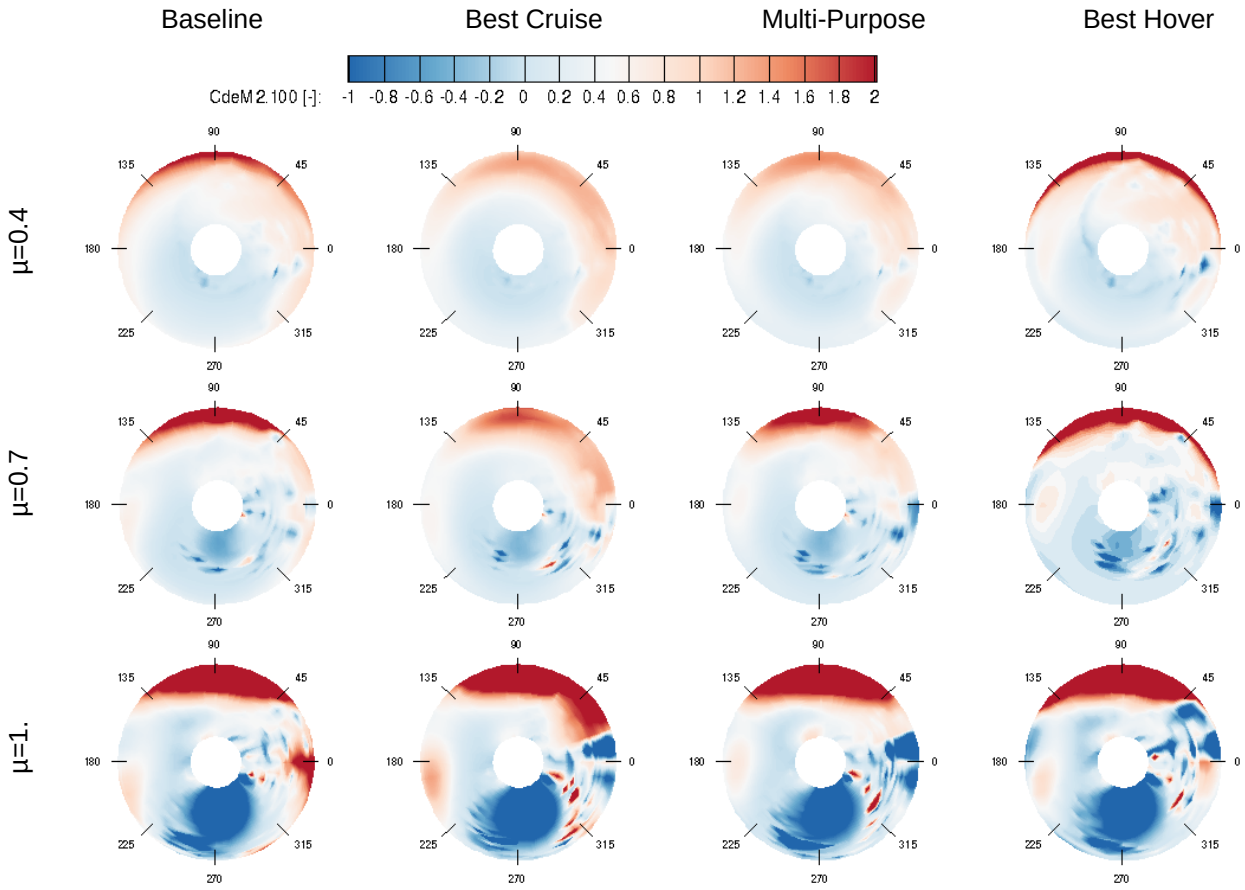

Figure 22: Effect of advance ratio on effective drag distribution on the rotor disk - c_T/σ =0.034 - LoFi - ONERA simulations

5. CONCLUSIONS

This paper summarizes the results obtained in the framework of the Work Package 3 of the JAXA-ONERA-DLR cooperation on rotor blades optimization. The aim of this study is to optimize the chord and the twist laws of the HART-II reference blade, to improve the aerodynamic performance in hover (for a high thrust c_T/σ=0.1), and in cruise (for a high advance ratio μ=0.7, due to a 50% RPM reduction, equivalent to a compound helicopter flight configuration). Each partner used its own optimization procedures, based on Kriging surrogate models, with different levels of fidelity.

Three designs in particular were studied: The Best Cruise, the Best Hover, and the Multi-Purpose, which can be determined by either a weighted objective function, or by a true multi-objective optimization procedure.

The main results from the three partners' optimization procedures can be summarized:

1. The Best Cruise designs present a thinner chord law in the inner and outer parts of the blades, balanced by a thickening in the middle section. The linear slope of the twist is close to zero. These optimized geometries allow an improvement of the effective lift-to-drag ratio, by a reduction of the lift and drag forces on the rotor disk in the right and left parts, and a new balance of the lift in the rear and aft areas. The wake generated by these Best Cruise blades has reduced vorticity intensity. The performances in hover of the Best Cruise designs are largely degraded, with an earlier stall occurrence.
2. The Best Hover designs allow a clear improvement of the Figure of Merit, in particular thanks to the reduction in twist to values that tend to be as negative as possible at the blade tip. This helps to delay the occurrence of stall. The wake of the Best Hover designs has much reduced vorticity intensity. The performances of the Best Hover designs are largely degraded in cruise.
3. The Multi-Purpose designs offer intermediate benefits / deficits between those of the Best Cruise and Best Hover designs. The chord laws are close to those of the Best Cruise designs.

The twist laws are between those of the Best Cruise and the Best Hover designs.

4. The utilization of a weighted objective function instead of a true multi-objective optimization still revealed a Pareto optimal design. While this cannot be generalized, this observation shows that a good balance between these two antagonistic goal functions of power in hover and forward flight can be found by simply combining them.

The next step could be to carry out cross-checking evaluations of the Best designs proposed by each partner, in an attempt to explain the differences observed locally. It would be also interesting to evaluate the performances of the LoFi designs by HiFi simulations, to quantify the accuracy contributions of the HiFi methods with respect to LoFi ones.

The next challenging optimization problem planned in the Work Package 4 will be to consider an acoustic objective function, to decrease the Blade Vortex Interaction noise level, for a descent flight configuration, by optimizing the chord, the twist and the sweep laws. Finally, the three objective functions (performance in hover, performance in cruise, and BVI noise level in descent) should be all considered all together.

Author contacts:

Joëlle Bailly: joelle.bailly-zibi@onera.fr

Gunther Wilke: gunther.wilke@dlr.de

Keita Kimura: kimura.keita@jaxa.jp

Yasutada Tanabe: tanabe.yasutada@jaxa.jp

6. REFERENCES

1. Bailly, J., and Bailly, D., "Multifidelity Aerodynamic Optimization of a Helicopter Rotor blade", *AIAA Journal*, Vol. 57, (8), 2019, pp. 3132-3144.

2. Wilke, G., "Variable-Fidelity Methodology for the Aerodynamic Optimization of Helicopter Rotors", AIAA Journal, Vol. 57, (8), 2019, pp. 3145-3158.

3. Sugiura, M., Tanabe, Y., Sugawara, H., and Takekawa, K., "Optimal Design of Rotor Blade for a winged Compound Helicopter at High Advance Ratio", American Helicopter Society 76th Annual Forum Proceedings, Virtual, 2020.

4. Sugiura, M., Tanabe, Y., Aoyama, T., Ortun, B., and Bailly, J., "An ONERA/JAXA Cooperative Research on the Assessment of Aerodynamic Methods for the Optimization of Helicopter Rotor Blades, Phase II", 42nd European Rotorcraft Forum Proceedings, Lille, France, 2016.

5. Van der Wall, B., G., "A Comprehensive Rotary-Wing Data Base for Code Validation: the HARTII International Workshop", *Aeronautical Journal*, 115, 2011, pp. 91-102.

6. Wilke, G., Bailly, J., Kimura, K., and Tanabe, Y., *"JAXA-ONERA-DLR Cooperation: Results from Rotor Optimization in Hover*", *CEAS Aeronautical Journal*, Vol. 13, (2), 2022, pp. 313-333.

7. Kimura, K., Wilke, G., Bailly, J., and Tanabe, Y., "JAXA-ONERA-DLR Cooperation: results from Rotor Optimization in forward Flight", 48th European Rotorcraft Forum, Winterthur, Switzerland, 2022.

8. Benoit, B., Dequin, A.M., Kampa, K., von Grünhagen, W., Basset, P.M., and Gimonet,B., "HOST, a General Helicopter Simulation Tool for Germany and France", American Helicopter Society 56th Annual Forum Proceedings, Virginia, 2000.

9. Basset, P.-M., Heuze, O., Prasad, J. V. R., Hamers, M., "Finite State Rotor Induced Flow Model for Interferences and Ground Effect", American Helicopter Society 57th Annual Forum Proceedings, Washington DC, 2001.

10. Toulmay, F., "Modele d'étude de l'aérodynamique du rotor," Rapport Eurocopter-France no R 371.376, 1986.

11. Bailly, J., Ortun, B., Delrieux, Y., Mercier des Rochettes, H., "Recent Advances in Rotor Aerodynamic Optimization, Including Structural Data Update", *Journal of the American Helicopter Society*, Vol. 62, 2017, pp.1–11.

12. Wilke, G., "Quieter and Greener Rotorcraft: Concurrent Aerodynamic and Acoustic Optimization", *CEAS Aeronautical Journal*, Vol. 12, 2021, pp. 495-508.

13. Maruyama, D., Bailly, D., and Carrier, G., "High-Quality Mesh Deformation using Quater-

nions for Orthogonality Preservation", *AIAA Journal*, Vol. 52, 2014, pp. 2712–2729.

14. Benoit, C., Perron, S., and Landier, S., "Cassiopee: A CFD Pre- and Post-Processing Tool", *Aerospace Science and Technology*, Vol. 45, 2015, pp. 272-283.
15. Allen, C.B., "CHIMERA Volume Grid Generation within the EROS Code", *Journal of the Aerospace Engineering*, Vol. 214 (3), 2000.
16. Cambier, L., Heib, S., and Plot, S., "The ONERA elsA CFD Software: Input from Research and Feedback from Industry", Mechanics & Industry, Vol. 14 (3), 2013, pp. 159-174.
17. Jochen, R., and Fassbender, J. K., "Block Structured Navier-Stokes Solver FLOWer", MEGAFLOW Numerical Flow Simulation for Aircraft Design," Springer, Berlin, Heidelberg, 2005, pp. 27-44.
18. Tanabe, Y., Saito, S., and Sugawara, H., "Validation of High Resolution CFD Analysis For Flowfield Around a Rotor", 40th JSASS Annual Meeting Proceedings, Japan, 2009.
19. Jameson, A., Schmidt, W., and Turkel, E., "Numerical Solution of the Euler Equations by Finite Volume Methods Using Runge & Kutta Time-Stepping Schemes", 4th AIAA Fluid and Plasma Dynamics Conference Proceedings, 1981.
20. Yamamoto, S., and Daiguji, H., "Higher Order-Accurate Upwind Schemes for Solving the Compressible Euler and Navier-Stokes Equations", *Computers and Fluids*, Vol. 22, Nos.2-3, 1993, pp.259-270.
21. Wilke, G., "New Results in Numerical and Experimental Fluid Mechanics", 1 ed., vol. XIII, Springer International Publishing, 2022, p. 790.
22. Kitamura, K., and Shima, E., "Towards Shock-Stable and Accurate Hypersonic Heating Computations: A New Pressure Flux for AUSM-Family Schemes" *Journal of Computational Physics*, Vol. 245, 2013, p. 62–83.
23. Yoon, S., and Jameson, A., "An LU-SSOR Scheme for the Euler and Navier-Stokes Equations," AIAA-1987-600, 1987.
24. Yoon, S., and Jameson, A., "Lower-Upper Symmetric-Gauss-Seidel Method for the Euler and Navier-Stokes Equations," *AIAA Journal*, Vol. 26, 1988, p. 1025–1026.
25. Kok, J., C., "Resolving the Dependence on Freestream Values for the k- Turbulence Model," *AIAA Journal*, Vol. 38, 2000, p. 1292–1295.
26. Dacles-Mariani, J., Kwak, D., and Zilliac, G., "On Numerical Errors and Turbulence Modeling in Tip Vortex Flow Prediction," *International Journal for Numerical Methods in Fluids*, Vol. 30, 1999, p. 65–82.
27. Heister, C. C., "A Method for Approximate Prediction of Laminar-Turbulent Transition on Helicopter Rotors," *Journal of the American Helicopter Society*, Vol. 63, 2018, p. 1– 14.
28. Jones, D.R., Schonlau, M., and Welch, W.J., "Efficient Global Optimization of Expensive Black-box Functions", *Journal of Global Optimization*, Vol. 13, 1998, pp. 455–492.
29. Kanazaki, M., Jeong, S., and Yamamoto, K., "High-Lift System Optimization based on the Kriging model using a High-Fidelity Flow Solver". Trans. Japanese Society for Aeronautical and Space Sciences, Vol. 49, 2006, pp. 169–174.
30. Kanazaki, M., Yokokawa, Y., Murayama, M., Ito, T., Jeong, S., and Yamamoto, K., "Nacelle Chine Installation Based on Wind-Tunnel Test using Efficient Global Optimization", Trans. Japanese Society of Aeronautical and Space Sciences, Vol. 51, 2008, pp. 146–150.
31. Kennedy, M.C., and O'Hagan, A., "Predicting the Output from a Complex Computer Code when Fast Approximations are Available", Biometrika 87, 2000, pp. 1–13.
32. Han, Z.-H., and Görtz, S., "A Hierarchical Kriging Model for Variable Fidelity Surrogate Modeling", AIAA Journal, Vol. 50, 2012, pp. 1885-1896.
33. Küfmann, P. M., Bartels, R., Van_Der_Wall, B. G., Schneider, O., Holthusen, H., and Gomes, J., "The First Wind Tunnel Test of The Multiple Swashplate System: Tesdure and Principal Results," Journal of the American Helicopter Society, Vol. 62 (4), 2017, pp. 1- 13.
34. Deb, K., Pratap, A., Agarwal, S. and Meyarivan, T., "A Fast and Elitist Multiobjective Ge-

netic Algorithm NSGA-II", *IEEE Transactions on Evolutionary Computation*, Vol. 6, (2), 2002, pp. 182-197.